Title: Processing of thermally stable 3D hierarchical ZIF-8@ZnO structures and their CO_2 adsorption studies

Author: Minju Thomas Balagopal N. Nair G.M. Anilkumar A. Peer Mohamed K.G.K. Warrier U.S. Hareesh

PII: S2213-3437(16)30043-4
DOI: http://dx.doi.org/doi:10.1016/j.jece.2016.01.043
Reference: JECE 966

To appear in:

Received date: 14-10-2015
Revised date: 7-1-2016
Accepted date: 31-1-2016

Please cite this article as: Minju Thomas, Balagopal N.Nair, G.M.Anilkumar, A.Peer Mohamed, K.G.K.Warrier, U.S.Hareesh, Processing of thermally stable 3D hierarchical ZIF-8@ZnO structures and their CO2 adsorption studies, Journal of Environmental Chemical Engineering http://dx.doi.org/10.1016/j.jece.2016.01.043

Processing of Thermally Stable 3D Hierarchical ZIF-8@ZnO Structures and their CO_2 Adsorption Studies

Minju Thomas, [a b]Balagopal N. Nair,*[c d] G. M. Anilkumar[c], A. Peer Mohamed,[a] K.G.K. Warrier[a] and U.S. Hareesh*[a,b]

[a]Material Science and Technology Division, National Institute for Interdisciplinary Science and Technology (CSIR-NIIST), Thiruvananthapuram-695019, India.

[b]Academy of Scientific and Innovative Research (AcSIR), New Delhi, India

[c]R&D Center, Noritake Co. Limited,300 Higashiyama, Miyoshi, Aichi 470-0293, Japan

[d]Nanochemistry Research Institute , Department of Chemistry, Curtin University, GPO Box UI987, Perth, WA6845, Australia

*Corresponding Authors:E-mail: hareesh@niist.res.in, bnair@n.noritake.co.jp

Fax: +0091 471 2491712; Tel: +0091 471 2535504

Graphical abstract

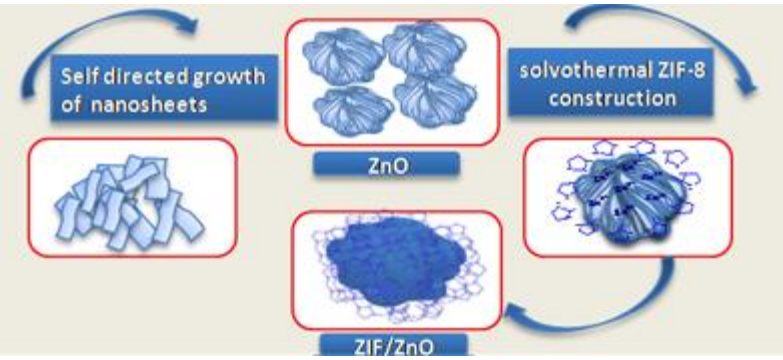

HIGHLIGHTS

- Solvothermal conversion of porous ZnO aggrgates to ZIF@ZnO coreshell structures
- Enhanced thermal stability by virtue of the ZnO core.
- Granules displayed CO_2 adsorption up to 0.33mmol/g at 25°C

ABSTRACT

Core-shell hybrid structures of ZnO-Zeolitic Imidazolate Framework-8 (ZIF@ZnO) were obtained by the solvothermal treatment of ZnO hierarchical structures having an average cluster size of ~3 μm and surface area of ~19 m^2/g. The surface area and pore volume of these supported structures could be tailored as a function of reaction time and temperature. Solvothermal treatment of ZnO structures in presence of imidazole at 95 °C for 24 h induced extremely large surface area of 733 m^2/g for the ZIF@ZnO samples. Samples thus obtained demonstrated a CO_2 adsorption capacity of 0.34 mmol/g at 25 °C compared to the value of 0.052 mmol/g measured for the ZnO structures. More significantly, the ZnO core helped the ZIF-8 surface fractal assemblies to significantly improve the thermal stability and retain their near spherical shapes allowing better handling in any practical adsorption application. The results validate that surface conversion of ZnO microstructures to ZIF-8 could be an efficient pathway towards the development of ZIF based supported adsorbents for CO_2 separation.

Keywords:Zeoliticimidazolate framework-8, Carbondioxide adsorption, Solvothermal reaction

1. Introduction

Zeoliticimidazolate frameworks (ZIF) are topological isomorphs of zeolites by virtue of the similarity in the metal-imidazole-metal angle of 145° with that of Si-O-Si angle. [1, 2] ZIFs also possess extremely good chemical and thermal stability [3-6]coupled with high surface area values. These desirable attributes of ZIF have recently attracted widespread interest and hence are being explored for a variety of applications ranging from molecular separation tocatalysis [7-10]. One of the major applications of ZIF-8 is the separation of carbon dioxide (CO_2) from flue gas streams to reduce carbon dioxide emissions to the atmosphere. Although, several materials are being investigated for this purpose [11-15] ZIFs, a typical member of Metal Organic Framework (MOF) family is considered as a candidate material for low temperature separation applications [16, 17].

Conventional methods of ZIF-8 synthesis employ solvothermal treatment of metallic zinc precursors in the presence of imidazole [3, 18, 19]. In addition, solvent free techniques like mechanochemical synthesis [20-22] were also employed for ZIF preparation. More recently, the use of metal oxides and hydroxides in place of metal salts enabled the formation of ZIF-8 as a surface layer of few nanometers thickness [23]. Alternatively, melting of low melting point ligands during the physical mixing with oxides/hydroxides present as salt offer solvent free method of ZIF-8 synthesis [24].

Functional materials consisting of ZIF-8 based hetero-structures are anticipated to impart significant advantages by virtue of the synergistic effects [25, 26]. Incorporation of carbon nanotubes (CNT) in to ZIF-8 was shown to improve the pore characteristics and the nanocomposites thus obtained showed enhanced carbon dioxide (CO_2) adsorption characteristics [27]. Fe_3O_4@ZIF-8magnetic core–shell microspheres demonstrated enhanced catalytic activity for the Knoevenagel condensation reaction of ethyl cyanoacetate and benzaldehyde [28]. The insitu growth of ZIF on polyurethane fibers, derived by electrospinning, was reportedfor fabricating air purifying clothes by virtue of their high surface area and CO_2capture [29]. Synthesis of highly stable ZIF-8 membrane on a macroporous alumina tube resulted in the development of a good molecular sieve of H_2 over CO_2 and CH_4[30]. Although several reports on processing of ZIF based adsorbents have been published, [31] the major issue that has limited the practical viability of ZIF is the absence of strategies that develop supported ZIF adsorbents. In fact, this concern is also highlighted in recent reviews on the

applications of MOFs and ZIFs necessitating the development of supported structures for wide spread practical applications in the field of adsorption, catalysis and membrane based separation [32, 33]. This is particularly important considering the fact that compaction processing of MOFs to monoliths often resulted in considerable reduction of surface area and loss of crystal structure [34]. It is therefore desirable to transform surface layers of self-supported aggregates of ZnO to ZIF enabling the development of asymmetric structures with controlled porosity on the transformed layer. The properties of membranes and adsorbents could be further improved by having a surface fractal structure with superior interface area between the solid surface and gas molecules.

The present work therefore explores the feasibility of converting porous aggregates of ZnO with relatively poor surface area into 3D hierarchical structures of extremely high surface area. Such ZIF@ZnO core shell structures are then demonstrated to show enhanced CO_2 adsorption characteristics compared to the precursor ZnO structures, while retaining the near spherical shape and uniform particle size characteristics. Improved thermal stability of the hybrid structures compared to pure ZIF-8 was another added advantage. It is shown that, the process route reported in this paper allows the development of stable and supported adsorbents of ZIF-8@ ZnO.

2. Experimental

2.1. Materials and Methods

2.1.1. Materials

Sodium hydroxide (97%, Merck, India) and Zinc nitrate hexahydrate (96%, Merck, India) for the synthesis of ZnO,2-methylimidazole (Sigma Aldrich, India). Methanol (Merck, India) and Distilled water as solvent

2.1.2. Synthesis of ZnO hierarchical structures

Aqueous solutions of Sodium hydroxide and Zinc nitrate hexahydrate (96%, Merck, India) in the molar ratio of 25:1 were mixed under constant magnetic stirring for two hours at room temperature. The suspension thus formed was further refluxed at 100 °C for one hour. The formed precipitate was filtered, washed five times with distilled water and dried in an air oven at 70 °C.

2.1.3 ZIF-8/ZnO (ZIF@ZnO) hybrid structures

1g of as prepared ZnO aggregates was dispersed in 30 mL methanol (Merck India). A solution of 2g 2-methylimidazole (Sigma Aldrich, India) in 220 mL

methanol (1:2 ratio) was added to the ZnO dispersion and the mixture was subjected to solvothermal treatment in a Teflon vessel for 24 h at 65 °C (sample denoted as ZIF@ZnO65). The precipitate was further washed three times with methanol and dried in a vacuum oven at 40 °C for 24 h. The influence of reaction time on the structure of ZIF@ZnO formed was evaluated at various synthesis durations of 6, 12, 24, 48 and 96 hours at the synthesis temperature of 65ºC. The temperature dependence of the formation of ZIF-8 was examined by varying the synthesis temperature from 65°C to 75°C and 95°C (samples denoted as ZIF@ZnO65, ZIF@ZnO75, and ZIF@ZnO95 respectively). The synthesis duration was fixed as 24 hours in all the above three cases. For comparison of porous structure, we have also prepared unsupported ZIF-8 as reported elsewhere[18]. For this, a solution of $Zn(NO_3)_2.6H_2O$ (2.933 g) in 200 mL methanol was mixed with a solution of 2-methylimidazole (HmIm) (6.489 g) in 200 mL of methanol under stirring at room temperature. After 1 h the formed particles were collected and washed with methanol and dried in a vacuum oven at 40 °C for 24 h.

2.2 Material characterization

CO_2 adsorption studies were performed on a BEL (Belsorpmax, BEL JAPAN INC) gas analyser. ZnO porous aggregates and the ZIF@ZnO hybrid structures were characterized by XRD for phase identification (PW1710 Philips, The Netherlands). Surface area and nitrogen adsorption-desorption measurements were performed using the previously described instrument (BEL) and surface area analyser (Micromeritics Gemini, USA). Thermo gravimetric analysis (TGA) was performed using a TGA apparatus (Perkin Elmer STA1000 TGA) in the temperature range of 30-800 °C at a heating rate of 5 ºC min^{-1}. TGA was also used to estimate the CO_2 adsorption capacity by the gravimetric method. Samples were first heated to 150 °C and CO_2 adsorption measurements were carried out after cooling to 50 °C. A CO_2 gas flow of 30 mL/min was maintained throughout the adsorption duration. Morphological features of samples prepared were obtained by scanning electron microscopic imaging (SEM, Carl Zeiss, Germany).Transmission electron microscopy (TEM) and high resolution TEM (HRTEM, Tecnai G2, FEI, The Netherlands, operated at 300 kV) images were also recorded for obtaining the finer details of the microstructures. The FTIR spectra were recorded on powders using Bruker αE FT-IR spectrometer.

3. Results and discussion

3.1 Phase analysis

The phase composition and crystallinity of "as prepared" ZnO aggregates, ZIF@ZnO65, ZIF@ZnO75and ZIF@ZnO95 hybrid structures are provided in the XRD patterns presented in Figure 1. The presence of (100), (002) and (101) peaks at 2 theta values between 30 and 40 confirmed the presence of hexagonal wurtzite phase in the ZnO aggregates (JCPDS 36-1451). The ZIF@ZnO hybrid structures provided peaks corresponding to (011), (002), (112), (022), (013), (222), (114), (233), (134) and (044) planes of ZIF-8 in addition to the peaks for ZnO. The XRD patterns of the samples obtained after solvothermal treatment of 65, 75 and 95 °C had one to one peak matching. The XRD patterns of samples obtained at different time intervals of solvothermal synthesis (at 65°C) are provided in Fig. S1.

3.2 Morphology and aggregate sizes

The SEM micrographs of the ZnO aggregates are presented in Fig. 2. The ZnO aggregates (Fig. 2a) were found to have a size distribution range of 1-5 µm with an average cluster size of ~ 3 µm. From the image analysis of 400 particles we found that the ZnO particles have a reasonable distribution of sizes with an average perimeter of 9.8 µm. The calculated average particle size from perimeter based on spherical geometry was 3.1 µm, whereas the average particle size calculated from area was only 1.8 µm. The perimeter based average particle size should have received good contribution from the very high surface roughness of the particles. The high magnification image of a single aggregate provided in Fig. 2b supported this observation and revealed the finer surface details of the 3D hierarchical structure as a self-assembly of closely packed nano sheets having thickness of ~50 nm. The stacking of the nano sheets obviously lead to a very rough surface when observed in the aggregate level.

The formation of ZnO from Zinc nitrate, in the presence of NaOH, could be described by the following reaction steps, [35]

$$Zn^{2+} + 2OH^{-} \rightarrow Zn(OH)_2 \quad (1)$$

$$Zn(OH)_2 \rightarrow Zn(OH)_4{}^{2-} \quad (2)$$

$$Zn(OH)_4{}^{2-} \rightarrow ZnO + 2H_2O + 2OH^{-} \quad (3)$$

In the absence of any surfactants and templates, the hierarchical structure formation is primarily ascribed to a concentration controlled kinetic phenomenon as reported by Li and Wang [35]. In the aqueous solution, due to the high concentration of OH^- ions the positively charged Zn (0001) plane allows faster growth along the $[01\bar{1}0]$leading to the formation of ZnO nanosheets with a$\{2\bar{1}\,\bar{1}0\}$ planar surface.

The SEM images of the ZnO porous aggregates after solvothermal treatment at 65°C and 95°C in 2-methylimidazole are presented in Fig. 3a-c. Without altering the spherical morphology and cluster sizes of aggregates, the imidazole (HmIm) treatment under solvothermal conditions provided the surface conversion of ZnO to ZIF-8 as evidenced microscopically by the partial smoothening of the aggregate surface. The formation of ZIF-8 has already been confirmed from the XRD data as reported earlier [36] and the reaction leading to its formation could be described by the following equation. The formation of ZIF@ZnO core-shell structures was reported to proceed by a mechanism involving the dissolution of ZnO in the basic imidazole solution followed by coordination with the de-protonated imidazolate anion [20].

$$ZnO + 2Hmim \rightarrow Zn(mIm)_2 + H_2O$$

3.3 Transmission Electron Microscopic Imaging

A closer look at the structure of ZIF@ZnO65 samples by TEM clearly indicated the development of ZIF-8 layer around the ZnO particles (Fig. 4a) without much disintegration of the original ZnO aggregates. The nano sheets of ZnO helped in the initial nucleation of ZIF-8 and as time increased more of HmIm is deprotonated resulting in the formation of a compact shell of ZIF-8 around the ZnO hierarchical structures. The TEM images of ZIF@ZnO65 structures at higher magnifications (Fig. 4b & c) clearly indicated the presence of needle like ZnO in the shell of ZIF-8 formed. When the temperature is further increased, the thickness of ZIF layer around the ZnO core was also more (Fig. 4e-f). A thickness of 50-100 nm was measured of the ZIF layer at 65°C while 200-300 nm of ZIF layer was obtained on increasing the temperature to 95 °C. The high resolution TEM image and the corresponding FFT of the sampleZIF@ZnO95 shown in figure 5 clearly confirmed the presence of ZIF-8 on ZnO. The (011), (002) planes of ZIF-8 along with the (002) planes of ZnO were identified from the FFT analysis. The HRTEM analysis testifies the formation of ZIF@ZnO heterostructures without the use of any additives and seeding procedures as has been reported elsewhere [37, 38]. The presence of ZnO needles in the ZIF-8 layer facilitated the heterostructure formation where dissolution of Zn^{2+} proceeded even after a complete ZIF layer formation leading to increased shell thickness with temperature. The slow reactivity of HmIm with Zn^{+} in methanol further allowed layer formation even in between the nanosheets as has been clearly seen in the TEM micrographs. It must be emphasized that the ZIF@ZnO structures retained

the spherical morphology and more or less the uniform particles sizes and could be thus be advantageous in their easy handling and usage for any practical sorption application.

3.4 *IR spectroscopy*

The phase analysis by XRD was also supported by the FTIR patterns presented in Fig.6 where characteristic peaks corresponding to ZIF-8 were identified on ZIF@ZnO samples after solvothermal treatment at the said temperatures and time. From FTIR it is clear that as synthesised ZIF@ZnO samples have same spectral characteristics as that of ZIF-8 and confirming thereby the formation of ZIF-8 above ZnO. The peak at 426 cm^{-1} is assigned for Zn-N stretching mode. The plane bending and stretching of the imidazole ring appeared in the spectral regions of 500-1350cm^{-1} and 1350-1500cm^{-1}, respectively. With increasing reaction temperatures the peak for Zn-O bond at 436 cm^{-1}shifted to 426 cm^{-1} for Zn-N (Fig. 6b).

3.5 Thermo gravimetric analysis

TGA was used to evaluate the formation of ZIF-8 with respect to reaction time and the results are shown in Fig. 7. As is evident from the figure, the decomposition of ZIF@ZnO65material under oxygen atmosphere started at around 380 ^{0}C and extended close to 450-500°C. The weight loss on heat treatment was directly proportional to the extent of ZIF-8 formation during the solvothermal treatment. The pure ZIF-8 under identical conditions recorded a weight loss of approximately 70% on heat treatment. The weight loss observed on ZnO porous aggregates is attributed to the adsorbed moisture and surface hydroxyl groups. The TGA results thus provided a quantitative estimation on the amount of ZIF-8 formed during solvothermal synthesis.

The thermo gravimetric analysis was done also on samples obtained at different solvothermal conditions (65-95°C). Fig 6a compares the decomposition profiles of such samples and it can be clearly seen that the amount of ZIF-8 formed has a direct dependence on the solvothermal temperature. Pure ZIF-8 retained ~35% of its total weight on heat treatment at 800°C while final weights of 77, 70,60 wt% are obtained for the samples of ZIF@ZnO at 65 , 75and 95°C respectively. The decomposition started at about 150°C for pure ZIF-8 and at about 380°C for ZIF@ZnO materials. Therefore, it can be observed that the starting decomposition temperature had a large delay in ZIF@ZnO structures and it can be concluded that the thermal stability of ZIF-8 supported by ZnO particles was considerably better compared to

unsupported samples. The enhanced thermal stability observed in ZIF@ZnO structures can be primarily ascribed to the presence of ZnO needles in the ZIF layer as a ceramic reinforcement. This heterostructure formation can significantly delay the break up and collapse of the ZIF framework structure around the ZnO core extending the thermal stability of such core shell structures. The enhanced thermal stability of ZIF@ZnO structures should be a significant advantage for increasing the temperature range of practical application of these materials as well as in terms of increased durability against failure while using in temperature swing adsorption cycles where desorption is carried above 100^{o}C.

3.6 BET Surface area values

The surface area (BET) and the pore volume measurements of ZIF@ZnO core-shell structures were evaluated using N_2 adsorption at liquid N_2 temperatures. N_2 adsorption isotherms of original ZnO powders and ZIF@ZnO65 are shown in Fig. 9. For comparison the isotherm measured on ZIF-8 powder samples is also included in the figure. The shape of isotherm corresponding to ZnO powders fits well with type IIb isotherm, These isotherms are obtained as a result of adsorption in the aggregates of plate-like particles. It is reported that, because of delayed capillary condensation, multilayer adsorption is able to proceed on the particle surface until a high P/P_o is reached. Once the condensation has occurred the state of the adsorbate will change and the desorption curve will therefore follow a different path thus developing hysterisis [40]due to the presence of aggregated structures.(separate isotherm is shown in the supplementary information fig:S2) evidencing the adsorption of nitrogen on ZnO particle surface. It should be noted that for an aggregate size of ~ 3 μm, the measured surface area value of 19 m^2/g is extremely high. Based on this measured surface area value of ZnO, the average particle size (assuming spherical shape) could be calculated as 56.3 nm. The high measured surface area value can therefore be ascribed to the unique morphology of the ZnO porous structures. As explained earlier, these structures are formed by the aggregation of nanosheets of ZnO of ~50 nm sizes and therefore such high surface area values should be ascribed to the surface structure (as the adsorption isotherm does not reveal porous structure). ZIF@ZnO65 hybrid structures as well as ZIF-8 samples showed microporous type adsorption presumably due to the Zeolitic type structure of ZIF-8 and are characterised by type I adsorption isotherms.

For comparison the adsorption isotherm of ZnO and ZIF-8 are also shown.

The surface area values of the ZIF@ZnO65 hybrid samples increased with increase in reaction time as shown in Fig. 10a. This is an obvious consequence of the increase in duration

of the reaction time leading to more ZIF around ZnO particles. For e.g. the 24 h sample showed a surface area value of 389 m^2/ g whereas the 96 h sample gave a value of 725 m^2/ g. Pore volume also increased with increase in reaction time, reaching 0.35cc/g for the 96 h (Fig. 10b).The micropore volume and micropore area calculated using the t plot method are given in the table (table ST1). The increase in microporous ZIF layer formation is again evidenced by the enhanced micropore volume and micropore area.

The isotherm and surface area values of the ZIF@ZnO hybrids with increasing solvothermal reaction temperature are shown in Fig. 9. The surface area values almost doubled as the temperature is increased from 65 to 95°C and is ascribed to the increased ZIF-8 formation as confirmed by thermal analysis as well as TEM measurements.The enhanced deprotonation and diffusion of Zn2+ at high temperatures help in the increased formation of micoporous ZIF-8 layer over ZnO aggregates resulting thereby in enhanced surface area.[41]

The results shown in Fig. 9-11indicated the growth of the porous ZIF-8 structure with reaction time and temperature and are complimentary to the results presented in Fig. 7b.The similarity of Figures 7b, 10a and 10b clearly supports the fact that the ZIF-8 is formed homogenously around the ZnO particles. Yet, it should also be noted that the curves in Figures 7(b), 10(a) and 10(b) show smoothening behaviour, possibly pointing to the limitations imposed on the progress of the reaction by the restricted Zn^{2+} transfer to the reaction interface through the already formed ZIF-8 shell.

3.7 CO_2 adsorption studies

Carbon dioxide adsorption isotherms, at 25 °C, of the samples ZnO, ZIF@ZnO65, ZIF@ZnO75 and ZIF@ZnO95 in comparison with the ZIF-8 powder samples are shown in Fig. 12. The ZnO porous aggregates displayed a low adsorption capacity of 0.052 mmol/g at 25 ^{0} C. ZIF@ZnO65 sample with a surface area of 389 m^2/g could adsorb 0.22 mmol/g CO_2 at 1 bar pressure. ZIF@ZnO75 samples adsorbed 0.28 mmol/g and ZIF@ZnO 95 sample having a surface area of 733 m^2/g adsorbed 0.34 mmol/g of CO_2 at 25^{o}C and 1 bar pressure. It is clear that the samples synthesized at higher reaction temperatures have increased CO_2 adsorption capacity by virtue of the higher surface area values obtained due to enhanced ZIF-8 formation.

The obtained volumetric adsorption capacity of ZIF is 0.7mmol/g [39] and that of ZIF@ZnO is 0.34mmol/g. The ZIF@ZnO 95 composite is only 60-70% ZIF(from TG data) and

therefore the adsorption capacity is only 20% less than pure ZIF when the mass is normalised. However, this limitation can be offset for practical application by the advantages obtained in terms of enhanced thermal stability and better flowability. Supported adsorbent structres always suffer from the inevitable deterioration of original adsorption capacity as the support part will not contribute to adsorption. However, our method has three benefits; support is an integral part of the system and ZIF layer is attached to it chemically. Therefore, we do not expect any breakage of the active adsorbent layer from the support. Secondly, although weak, the support layer also contribute some amount of adsorption as it is also porous. Thirdly, as the support here take part in the reaction forming the shell, the size of the core and shell could be controlled easily to optimize the adsorption capacity Vs. mechanical strength. A large core of ZnO will be better in terms of strength whereas a thick shell of ZIF will be better in terms of adsorption capacity.

The kinetics of CO_2 adsorption of ZIF@ZnO samples was measured by gravimetric method at 50 $^{\circ}$C and results are shown in the supplementary information. From the gravimetric adsorption curves shown in Fig. S3, the kinetics of adsorption (corresponding to 50% of adsorption capacity) could be calculated as in Table 1

The tabulated data clearly indicated an increase in adsorption rate with increased ZIF-8 formation. However it should be noted that the values are meant only as representative, as the coverage value was different between the samples. Furthermore, the isosteric heat of adsorption was derived from the adsorption curves obtained at 5 °C (Fig. S4) and 25 °C (Fig. 10) for the ZIF@ZnO65 sample. At the surface coverage values of 0.04 mmol/g, 0.14 mmol/g and 0.22 mmol/g heats of adsorption values could be calculated as 13.8 kJ/mol, 14.0 kJ/mol and 14.4 kJ/mol respectively. The heat of adsorption values were found reasonable compared to the values reported in literature [27]

4. Conclusions

ZnO hierarchical structures having a fractal surface morphology were directly converted to ZeoliticImidazolate Framework-8 (ZIF-8)-ZnO hybrid structures. ZnO aggregates with an average cluster size of ~3 μm and surface area of ~19 m^2/g were used resulting in ZIF@ZnO surface fractal assemblies with microporous structure. The surface conversion of ZnO to ZIF was largely influenced by the solvothermal reaction temperature. The core-shell type hybrid structure synthesized solvothermally at 95°C for 24 h produced ZIF@ZnO core shell materials having a surface area of 733 m^2/g and CO_2 adsorption

capacity of 0.34 mmol/g at 25 °C. ZIF@ZnO supported structures were found thermally stable up to 380°C compared to the thermal stability of 150 °C measured for ZIF-8 unsupported samples. ZIF@ZnO supported samples also had uniform spherical shape facilitating better handling and packing in adsorption applications. It can be concluded that the surface conversion of ZnO to ZIF-8 thus provides an efficient pathway for the development of supported adsorbents of ZIF-8 for CO_2 separation.

Acknowledgements

The authors acknowledge the Council of Scientific and Industrial Research (CSIR), New Delhi, India, and Noritake Co. Limited, Aichi, Japan, for providing research facilities and financial support (CLP218739).

Appendix A. Supplementary data

References

[1] J.P. Zhang, Y.B. Zhang, J.B. Lin, X.-M. Chen, Metal Azolate Frameworks: From Crystal Engineering to Functional Materials, Chem.Rev 112 (2011) 1001-1033.

[2] J. Perez-Pellitero, H. Amrouche, F.R. Siperstein, G. Pirngruber, C. Nieto-Draghi, G. Chaplais, A. Simon-Masseron, D. Bazer-Bachi, D. Peralta, N. Bats, Adsorption of CO2, CH4, and N-2 on Zeolitic Imidazolate Frameworks: Experiments and Simulations, Chem. Eur. J 16 (2010) 1560-1571.

[3] K.S.N. Park, A.P.C. Zheng Cote, Jae Yong, R. Huang, F.J. Uribe-Romo, H.K. Chae, M. O'Keeffe, O.M. Yaghi, Exceptional chemical and thermal stability of zeolitic imidazolate frameworks, Proc.Natl. Acad. Sci. U. S. A. 103 (2006) 10186-10191.

[4] J.P. Zhang, A.X. Zhu, R.-B. Lin, X.L. Qi, X.-M. Chen, Pore Surface Tailored SOD-Type Metal-Organic Zeolites, Adv. Mater. 23 (2011) 1268-1271.

[5] P. Kusgens, M. Rose, I. Senkovska, H. Frode, A. Henschel, S. Siegle, S. Kaskel, Characterization of metal-organic frameworks by water adsorption, Microporous Mesoporous Mater. 120 (2009) 325-330.

[6] R. Galvelis, B. Slater, R. Chaudret, B. Creton, C. Nieto-Draghi, C. Mellot-Draznieks, Impact of functionalized linkers on the energy landscape of ZIFs, Crystengcomm 15 (2013) 9603-9612.

[7] L.H. Wee, N. Janssens, S.P. Sree, C. Wiktor, E. Gobechiya, R.A. Fischer, C.E.A. Kirschhock, J.A. Martens, Local transformation of ZIF-8 powders and coatings into ZnO nanorods for photocatalytic application, Nanoscale 6 (2014) 2056-2060.

[8] S. Xian, F. Xu, C. Ma, Y. Wu, Q. Xia, H. Wang, Z. Li, Vapor-enhanced CO2 adsorption mechanism of composite PEI@ZIF-8 modified by polyethyleneimine for CO_2/N_2separation, Chem. Eng. J. 280 (2015) 363-369.

[9] J. Zheng, C. Cheng, W.J. Fang, C. Chen, R.W. Yan, H.X. Huai, C.C. Wang, Surfactant-free synthesis of a Fe3O4@ZIF-8 core-shell heterostructure for adsorption of methylene blue, Crystengcomm 16 (2014) 3960-3964.

[10] C.H. Kuo, Y. Tang, L.Y. Chou, B.T. Sneed, C.N. Brodsky, Z. Zhao, C.K. Tsung, Yolk-Shell Nanocrystal@ZIF-8 Nanostructures for Gas-Phase Heterogeneous Catalysis with Selectivity Control, J Am. Chem. Society 134 (2012) 14345-14348.

[11] C. Chen, J. Kim, D.A. Yang, W.S. Ahn, Carbon dioxide adsorption over zeolite-like metal organic frameworks (ZMOFs) having a sod topology: Structure and ion-exchange effect, Chem. Eng. J 168 (2011) 1134-1139.

[12] T.F. José D. Figueroaa, Sean Plasynskia, Howard McIlvriedb, Rameshwar D. Srivastavab, Advances in CO2 capture technology-The U.S. Department of Energy's Carbon Sequestration Program, Int. J. Greenh. Gas Control. 2 (2008) 9-20.

[13] P.V. Subha, B.N. Nair, P. Hareesh, A.P. Mohamed, T. Yamaguchi, K.G.K. Warrier, U.S. Hareesh, Enhanced CO_2 absorption kinetics in lithium silicate platelets synthesized by a sol-gel approach, J. Mater. Chem. A 2 12792-12798.

[14] B.N. Nair, R.P. Burwood, V.J. Goh, K. Nakagawa, T. Yamaguchi, Lithium based ceramic materials and membranes for high temperature CO2 separation, Prog. Mater. Sci. 54 (2009) 511-541.

[15] P.V. Subha, B.N. Nair, P. Hareesh, A.P. Mohamed, T. Yamaguchi, K.G.K. Warrier, U.S. Hareesh, CO2 Absorption Studies on Mixed Alkali Orthosilicates Containing Rare-Earth Second-Phase Additives, The J. Phys. Chem. C 119 (2015) 5319-5326.

[16] Y.S. Bae, R.Q. Snurr, Development and Evaluation of Porous Materials for Carbon Dioxide Separation and Capture, Angew. Chem. Int. Ed. 50 (2011) 11586-11596.

[17] N. Hara, M. Yoshimune, H. Negishi, K. Haraya, S. Hara, T. Yamaguchi, ZIF-8 membranes prepared at miscible and immiscible liquid-liquid interfaces, Microporous Mesoporous Mater. 206(2015) 75-80.

[18] J. Cravillon, C.A. Schroder, H. Bux, A. Rothkirch, J. Caro, M. Wiebcke, Formate modulated solvothermal synthesis of ZIF-8 investigated using time-resolved in situ X-ray diffraction and scanning electron microscopy, Crystengcomm 14 (2012) 492-498.

[19] Y.R. Lee, M.S. Jang, H.Y. Cho, H.-J. Kwon, S. Kim, W.-S. Ahn, ZIF-8: A comparison of synthesis methods, Chem. Eng. J 271(2015) 276-280.

[20] S. Tanaka, K. Kida, T. Nagaoka, T. Ota, Y. Miyake, Mechanochemical dry conversion of zinc oxide to zeolitic imidazolate framework, Chem.Commun. 49 (2013) 7884-7886.

[21] M.J. Cliffe, C. Mottillo, R.S. Stein, D.-K. Bucar, T. Friscic, Accelerated aging: a low energy, solvent-free alternative to solvothermal and mechanochemical synthesis of metal-organic materials, Chemical Sci. 3 (2012) 2495-2500.

[22] S.L. James, C.J. Adams, C. Bolm, D. Braga, P. Collier, T. Friscic, F. Grepioni, K.D.M. Harris, G. Hyett, W. Jones, A. Krebs, J. Mack, L. Maini, A.G. Orpen, I.P. Parkin, W.C. Shearouse, J.W. Steed, D.C. Waddell, Mechanochemistry: opportunities for new and cleaner synthesis, Chem. Soc. Rev. 41 (2012) 413-447.

[23] I. Stassen, N. Campagnol, J. Fransaer, P. Vereecken, D. De Vos, R. Ameloot, Solvent-free synthesis of supported ZIF-8 films and patterns through transformation of deposited zinc oxide precursors, Crystengcomm 15 (2013) 9308-9311.

[24] J.B. Lin, R.B. Lin, X.N. Cheng, J.-P. Zhang, X.-M. Chen, Solvent/additive-free synthesis of porous/zeolitic metal azolate frameworks from metal oxide/hydroxide, Chem.Commun. 47 (2011) 9185-9187.

[25] L. Lin, T. Zhang, H. Liu, J. Qiu, X. Zhang, In situ fabrication of a perfect Pd/ZnO@ZIF-8 core-shell microsphere as an efficient catalyst by a ZnO support-induced ZIF-8 growth strategy, Nanoscale 7 (2015) 7615-7623.

[26] N. Wang, G. Shi, J. Gao, J. Li, L. Wang, H. Guo, G. Zhang, S. Ji, MCM-41@ZIF-8/PDMS hybrid membranes with micro- and nanoscaled hierarchical structure for alcohol permselective pervaporation, Sep. Purif. Technol. 153(2013) 146-155.

[27] Y. Yang, L. Ge, V. Rudolph, Z. Zhu, In situ synthesis of zeolitic imidazolate frameworks/carbon nanotube composites with enhanced CO_2 adsorption, Dalton Trans. 43 (2014) 7028-7036.

[28] T. Zhang, X. Zhang, X. Yan, L. Kong, G. Zhang, H. Liu, J. Qiu, K.L. Yeung, Synthesis of Fe_3O_4@ZIF-8 magnetic coreshell microspheres and their potential application in a capillary microreactor, Chem. Eng. J 228(2013) 398-404.

[29] Z. Lian, L. Huimin, O. Zhaofei, In situ crystal growth of zeolitic imidazolate frameworks (ZIF) on electrospun polyurethane nanofibers, Dalton Trans. 43 (2014) 6684-6688.

[30] L. Kong, X. Zhang, H. Liu, J. Qiu, Synthesis of a highly stable ZIF-8 membrane on a macroporous ceramic tube by manual-rubbing ZnO deposition as a multifunctional layer, J. Membrane Sci.490 354-363.

[31] B. Yu, F. Wang, W. Dong, J. Hou, P. Lu, J. Gong, Self-template synthesis of core shell ZnO@ZIF-8 nanospheres and the photocatalysis under UV irradiation, Mater. Lett.156 (2015) 50-53.

[32] J. Gascon, A. Corma, F. Kapteijn, F.X. Llabrés i Xamena, Metal Organic Framework Catalysis: Quo vadis?ACS Catal. 4 (2014) 361-378.

[33] B. Chen, Z. Yang, Y. Zhu, Y. Xia, Zeolitic imidazolate framework materials: recent progress in synthesis and applications, J. Mater. Chem. A 2 (2014) 16811-16831.

[34] C. Montoro, F. Linares, E.Q. Procopio, I. Senkovska, S. Kaskel, S. Galli, N. Masciocchi, E. Barea, J.A. Navarro, J. Am. Chem. Soc. 133 (2011) 11888.

[35] B. Li, Y. Wang, Facile Synthesis and Enhanced Photocatalytic Performance of Flower-like ZnO Hierarchical Microstructures, The J. Phy. Chem. C 114 (2009) 890-896.

[36] S.R. Venna, M.A. Carreon, Highly Permeable Zeolite Imidazolate Framework-8 Membranes for CO_2/CH_4 SeparationRecord NumberJ. Am. Chem. Soc. 132 (2009) 76-78.

[37] Y.n. Wu, M. Zhou, B. Zhang, B. Wu, J. Li, J. Qiao, X. Guan, F. Li, Amino acid assisted templating synthesis of hierarchical zeolitic imidazolate framework-8 for efficient arsenate removal, Nanoscale 6 (2014) 1105-1112.

[38] S. Sorribas, B. Zornoza, C. Tellez, J. Coronas, Ordered mesoporous silica-(ZIF-8) core-shell spheres, Chem. Commun. 48 (2012) 9388-9390.

[39] S. Gadipelli, W. Travis, W. Zhou, Z. Guo, A thermally derived and optimized structure from ZIF-8 with giant enhancement in CO_2 uptake, Energy Environ. Sci. 7 (2014) 2232-2238.

[40] F.Rouquerol, J Rouquerol, K.Sing, Adsorption by Powders and Porous Solids, Academic Press, London ,1999

[41] M. Lanchas, D. Vallejo-Sanchez, G. Beobide, O. Castillo, A.T. Aguayo, A. Luque, P. Roman, A direct reaction approach for the synthesis of zeolitic imidazolate frameworks: template and temperature mediated control on network topology and crystal size, Chem.Commun. 48 (2012) 9930-9932.

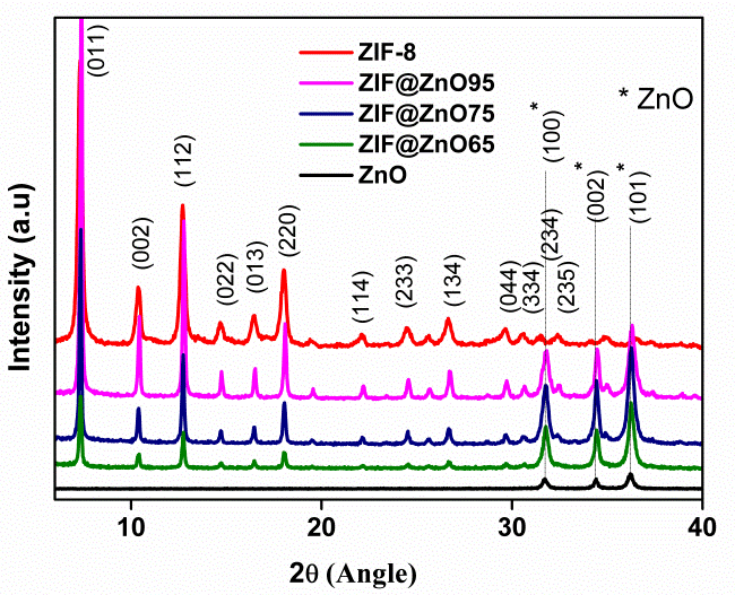

Fig. 1. XRD patterns of ZnO porous aggregates and ZIF@ZnO made at different reaction temperatures in comparison with pure ZIF-8

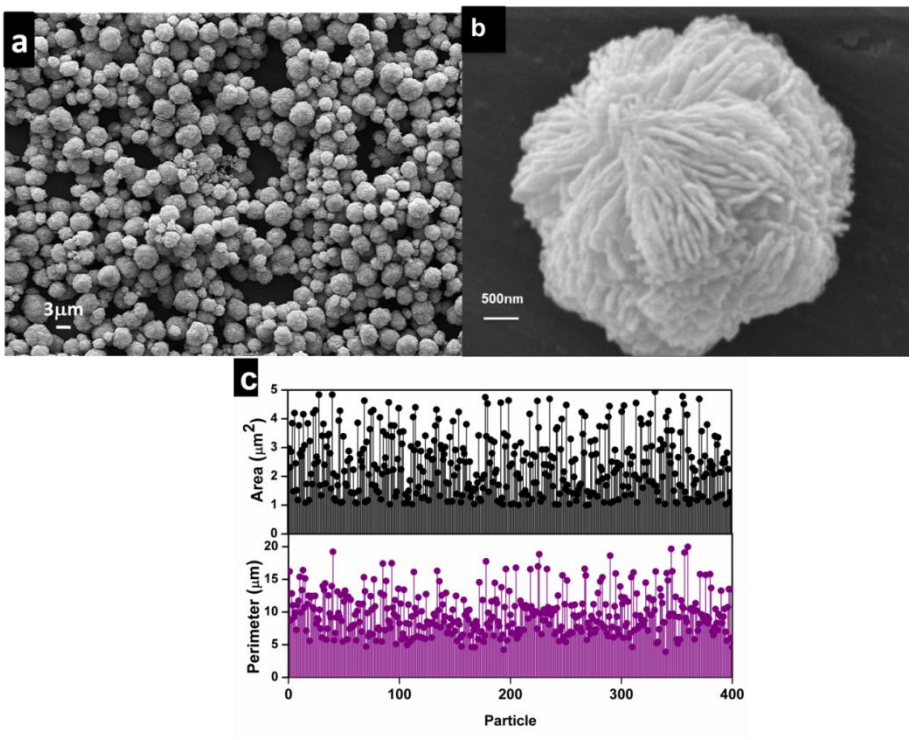

Fig. 2.SEM micrographs of a) Porous ZnO aggregates b) One of the larger particle at higher magnification c) Size distribution based on the image analysis of 400 particles

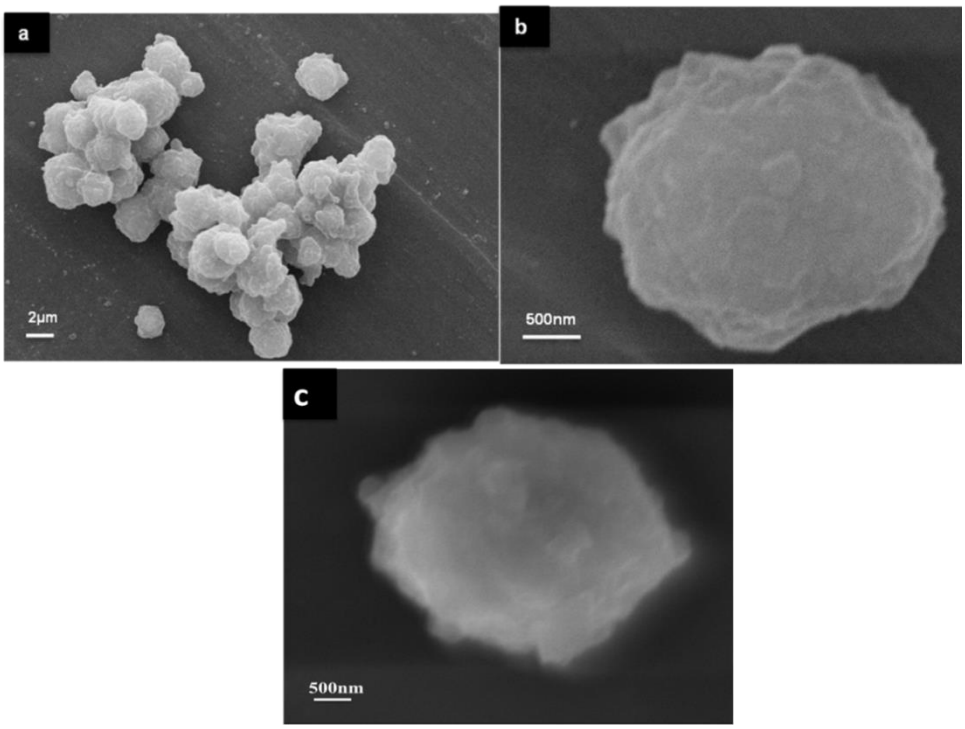

Fig. 3.SEM micrographs of a) ZIF@ZnO65 hybrid structures b) ZIF@ZnO65 hybrid structures at higher magnification c) ZIF@ZnO95 hybrid structures at higher magnification

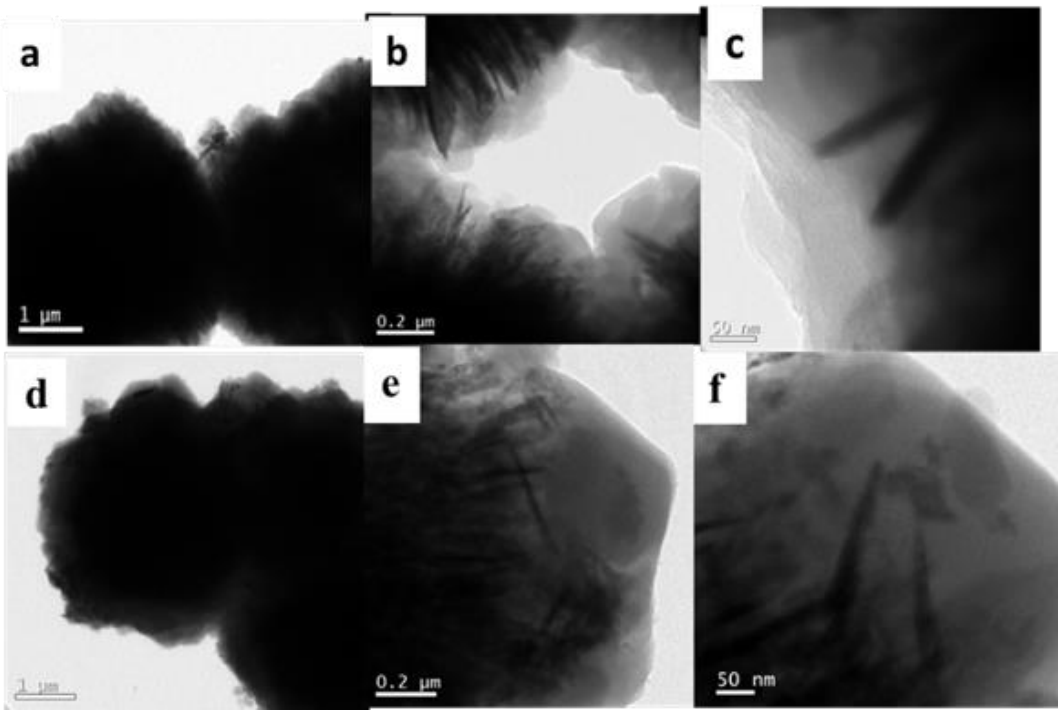

Fig. 4.ZIF@ZnO hybrid structures as observed by TEM at low, medium and high magnifications (a-c) ZIF@ZnO65 and (d-f) ZIF@ZnO95

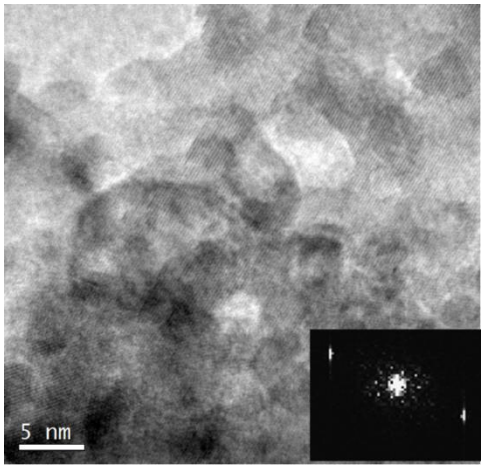

Fig.5.a) HRTEM image of ZIFZnO95 and corresponding FFT in inset

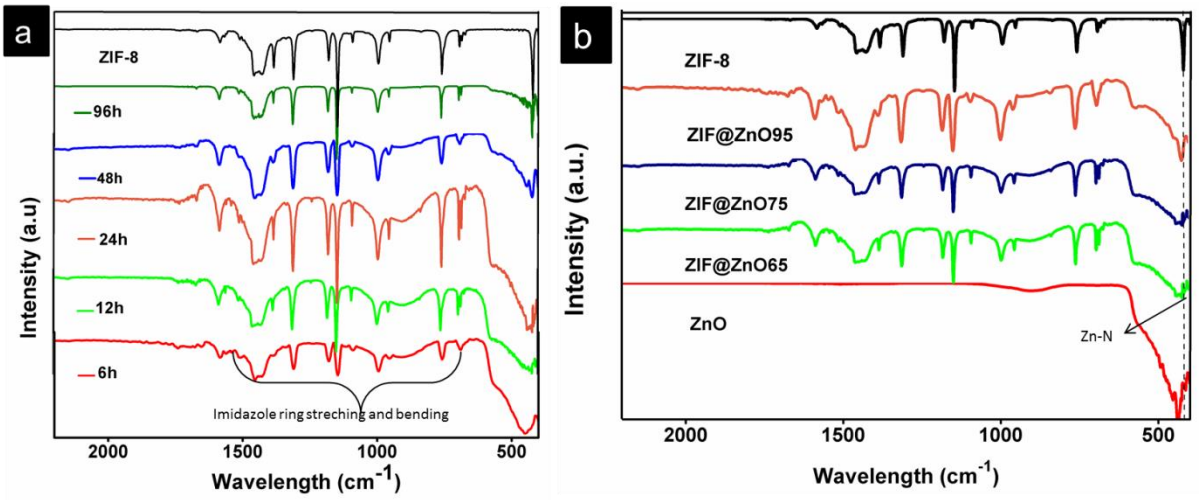

Fig.6.The FTIR patterns of the a) ZIF-8 and ZIF-8@ZnO samples at different reaction times b) ZIF-8 ,ZIF-8@ZnO samples at different reaction temperatures and ZnO

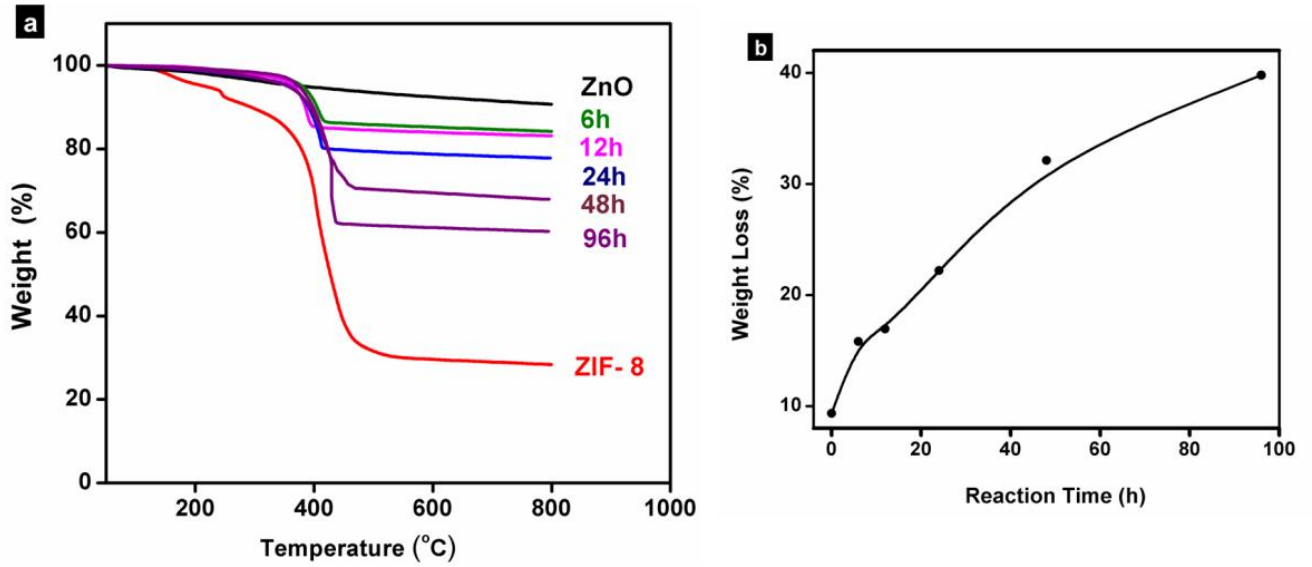

Fig. 7. a) Thermal analysis curves of ZIF@ZnO65 samples corresponding to various reaction times. For comparison TGA curves of ZIF-8 powder samples are also shown b) percentage weight reduction with respect to reaction time of ZIF@ZnO samples.

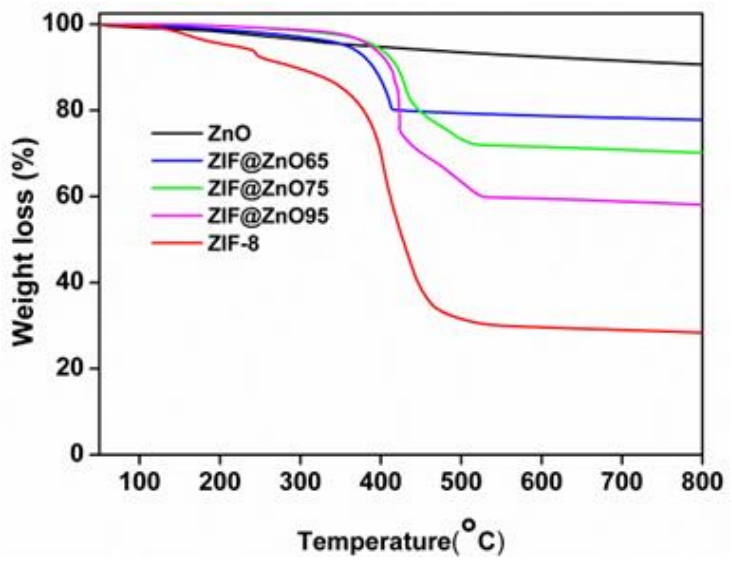

Fig. 8. Thermal analysis curves of ZIF@ZnO samples corresponding to various reaction temperatures. For comparison TGA curves of ZIF-8 powder samples are also shown

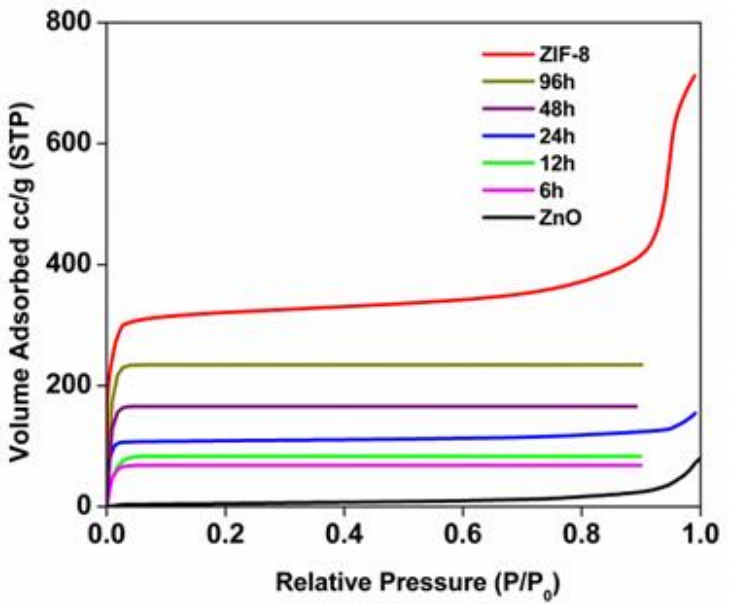

Fig.9. Nitrogen adsorption isotherms of ZIF@ZnO65 samples made at different reaction times.

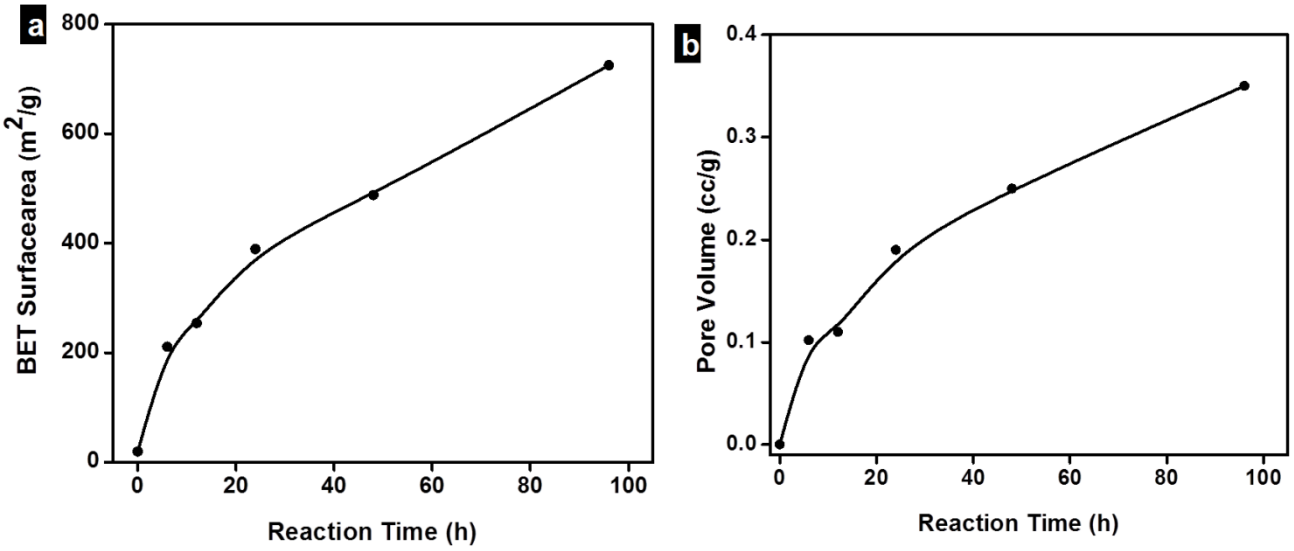

Fig. 10. a) BET surface area b) Pore volume of the ZIF@ZnO65 samples corresponding to different reaction times.

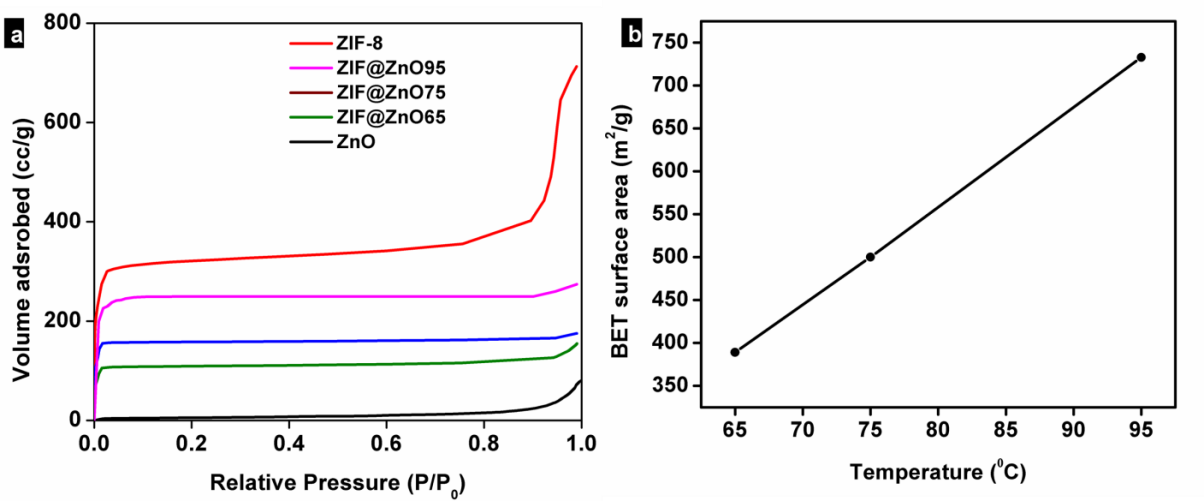

Fig. 11. a) Nitrogen adsorption isotherms of ZnO, ZIF@ZnO samples as well as ZIF-8 b)The change in surface area of ZIF@ZnO with synthesis temperature is represented using surface area values of ZIF@ZnO65, ZIF@ZnO75 and ZIF@ZnO95

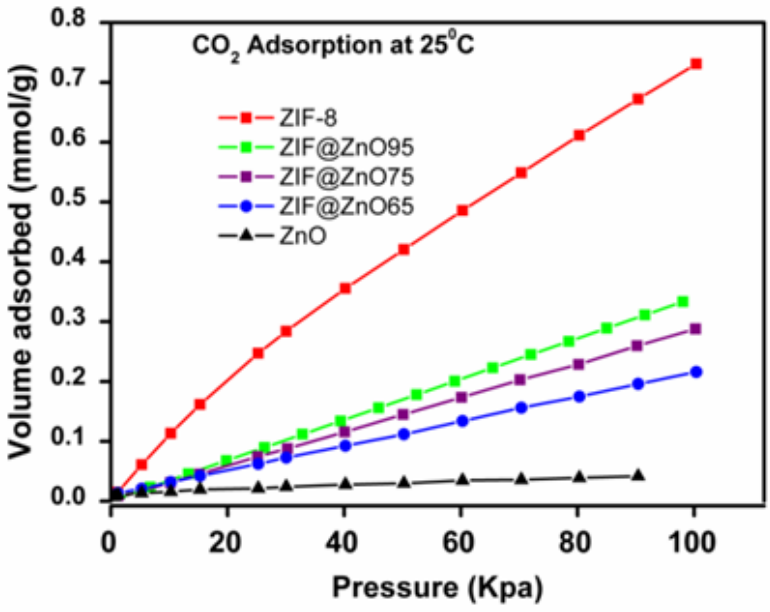

Fig. 12. Carbon dioxide adsorption isotherms of ZnO, ZIF@ZnO65, ZIF@ZnO75,ZIF@ZnO 95 and ZIF-8 at 25°C.

Table 1: Adsorption rate of ZIF@ZnO hybrid structures compared with ZIF-8 based on gravimetric adsorption data

No	Sample	Adsorption Rate (mmol/g.s)
1	ZIF@ZnO65	4.6x10-4
2	ZIF@ZnO75	9.0x10-4
3	ZIF@ZnO95	1.2x10-3
4	ZIF-8	3.2 x10-3